

質に対して重量比で8:1加えること、再水和時においては少量の水を連続的に添加すること、ピラルビシンの封入にはリポソーム脂質成分としてオレイン酸を添加することが必要であることを明らかにした。リポソームの膜構造は凍結乾燥によって破壊され、再水和時に再構築が起きて、そのとき水に溶解した薬物がリポソーム内に進入すると推察した。糖の脂質への分子運動性に対する影響は糖と脂質との比によって異なり、その比が高いとリポソームの脂質膜を安定化し、その比が低いと膜の透過性を高めることが示唆された。

F. 学会発表

川野久美、高山幸三、永井恒司、米谷芳枝、ピラ

ルビシン封入肝ターゲティングリポソーム製剤の調製と評価、日本薬剤学会第17年会(静岡)、2002年3月予定

K. Kawano, K. Takayama, T. Nagai, G. Gregoriadis, Y. Maitani, Preparation and antitumor effects of pirarubicin-encapsulating liposomes for liver cancer treatment, the Controlled Release Society 29th annual meeting, 2002, July, Korea.

Table 1 The effect of sugar on the average particle size and entrapment efficiency of SL-THP at sugar/lipid=1 (w/w).

EPC : Ch : Sit-G : OA (molar ratio)	Sugar	Average particle size (nm)	Entrapment efficiency (%)
7 : 3 : 2 : 0	Without sugar	1317.1	31.2
	Glucose	187.3	26.8
	Lactose	389.5	30.7
	Sucrose	147.2	34.9
7:3:2:1	Without sugar	1244.7	80.0
	Glucose	675.5	87.3
	Lactose	1245.4	78.6
	Sucrose	780.4	71.5

Table 2 The effect of sucrose ratio to lipid on the average particle size and entrapment efficiency of THP.

EPC : Ch : Sit-G : OA (molar ratio)	Sucrose/ Lipid (w/w)	Average particle size (nm)	Entrapment efficiency (%)
7:3:2:1	0	979.0 ± 129.6	81.0 ± 6.0
	2	423.7 ± 35.8	82.4 ± 10.7
	5	412.4 ± 1.5	82.6 ± 4.9
	8	341.0 ± 41.1	80.7 ± 11.3

Table 3 The average particle size and entrapment efficiency of liposomes after sonication.

EPC : Ch : Sit-G : OA (molar ratio)	Particle size (nm)	Entrapment efficiency (%)
7:3:2:1	197.8	84.6
7:5:1	168.6	82.7



(a)

(b)

(c)

Fig. 1 Scanning electronic micrograph of EPC:Ch:Sit-G:OA=7:3:2:1 (molar ratio). (a) Freeze-dried liposomes without sucrose. (b) Freeze-dried liposomes with sucrose. (c) Rehydrated liposomes freeze-dried with sucrose.

研究成果の刊行に関する一覧表
雑誌

発表者氏名	論文タイトル名	発表誌名	巻名	ページ	出版年
Yoshioka, S., Aso, Y. and Kojima, S	Usefulness of the Kohlrausch-Williams-Watts Stretched Exponential Function to Describe Protein Aggregation in Lyophilized Formulations and the Temperature Dependence Near the Glass Transition Temperature	<i>Pharm.Res.</i>	18	256-260	2001
Aso, Y., Yoshioka, S and Kojima, S	Feasibility of using isothermal microcalorimetry to evaluate the physical stability of amorphous nifedipine and phenobarbital	<i>Thermochimica Acta</i>	380	199-204	2001
Aso, Y., Yoshioka, S and Kojima, S	Explanation of the crystallization rate of amorphous nifedipine and phenobarbital from their molecular mobility as measured by ¹³ C nuclear magnetic resonance relaxation time and the relaxation time obtained from the heating rate dependence of the glass transition temperature	<i>J.Pharm.Sci</i>	90	798-806	2001
N. Murase, M. Ruike, N. Matsunaga, M. Hayakawa, Y. Kaneko and Y.Ono	Spider silk has an ice nucleation activity	Naturwissenschaften	88	117-118	2001
K. Kajiwara, A. Motegi and N. Murase	Freeze-thawing behaviour of highly concentrated aqueous alkali chloride-flucose systems	Cryo-Letters	22	311-320	2001
村勢則郎	凍結高分子ゲル中の水の物理状態、	冷凍	77	44-48	2001
村勢則郎、堀江誠、小林智恵美、楊井洋子、梶原一人、渡部徳子	:凍結濃縮によるデキストラン-KCl 水溶液の可逆的ゲル化	低温生物工学会誌,	47	31-33	2001
Wang J., Y. Maitani, K. Takayama and T. Nagai	In vivo evaluation of doxorubicin carried with long circulating and remote loading proliposome	Int. J. Pharm.	219	183-184	2001
K. Muramatsu, Y. Maitani, S. H. Hwang, S. Tanaka, K. Takayama and T. Nagai	Physicochemical characteristics and transfection efficiency of DNA in cationic and neutral liposomes with soybean-derived sterylglucoside into HepG2 cells	J. Pharm. Sci. Technol. Jpn.	61	1- 10	2001
Y. Maitani, H. Soeda, W. Junping and K. Takayama	Modified ethanol injection method for liposomes containing b-sitosterol b-D-glucoside	J. Liposome Res.	11	115-125	2001

発表者氏名	論文タイトル名	発表誌名	巻名	ページ	出版年
Y. Maitani, K. Kawano, K. Yamada, T. Nagai and K. Takayama	Efficiency of liposomes surface-modified with soybean-derived sterylglucoside as a liver targeting carrier in HepG2 cells	J. Contr. Release;	75	381-389	2001
S. H. Hwang, K. Takayama and Y. Maitani,	Liver-targeted gene transfer into a human hepatoblastoma. cell line and in vivo by sterylglucoside -containing cationic liposomes	Gene Therapy	8	1276-80	2001

GLASS TRANSITION AND ICE CRYSTALLISATION OF WATER IN POLYMER GELS STUDIED BY OSCILLATION DSC, XRD-DSC SIMULTANEOUS MEASUREMENTS AND RAMAN SPECTROSCOPY

Norio MURASE, Masatoshi RUIKE, Sumie YOSHIOKA*, Chihiro KATAGIRI** and Hiroshi TAKAHASHI***

Department of Biotechnology, School of Science and Engineering, Tokyo Denki University, Hiki-gun, Saitama 350-0394, *National Institute of Health Sciences, Setagaya-ku, Tokyo 158-8501, **Institute of Low Temperature Sciences, Hokkaido University, Sapporo 060-0819, ***Faculty of Engineering, Gunma University, Maebashi-shi 371-8510, JAPAN.

1 INTRODUCTION

Water in polymer gels of a certain density of crosslink is considered to remain partially unfrozen during freezing and to turn into a glassy state, which undergoes ice crystallisation during rewarming. The consideration is supported by the fact that the amount of unfrozen water, estimated by DSC, is more with the gel than the other gels different only in the crosslink density¹. However, glass transition has not yet been detected with the gel. In this connection, DSC rewarming trace shows an endothermic trend prior to the exotherm due to ice crystallisation. Origin of the trend is unclear; whether it is due to the melting of small ice crystal where the melting temperature is partially depressed by Kelvin effect or it is due to glass transition with some enthalpy relaxation¹⁻³. A typical DSC rewarming trace indicating such behaviour is shown in Figure 1 for the reference.

The characteristic behaviour of the DSC rewarming trace should be rationally explained by the corresponding physical events occurring in the gel. For the clarification of the mechanism of glass transition as well as ice crystallisation during rewarming, oscillation DSC, XRD (X-ray diffraction) - DSC simultaneous measurements were performed in this study. Raman

spectroscopic studies were also carried out to obtain further information about the frozen state of the gel. (Figure 1)

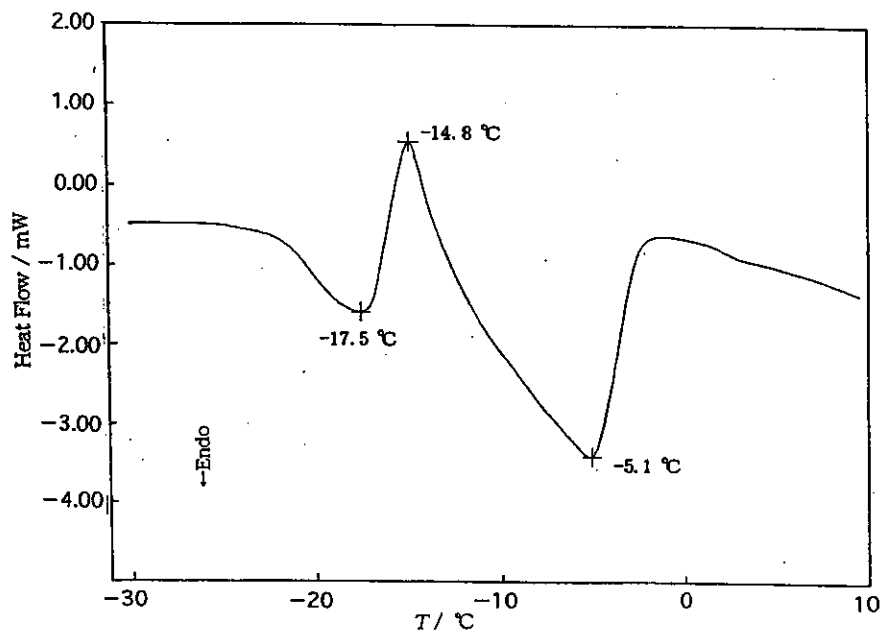


Figure 1 A typical DSC heating trace obtained with a frozen Sephadex G25 gel containing 50 wt% water. Cooling and heating rates were $10\text{ }^{\circ}\text{C min}^{-1}$ and $3\text{ }^{\circ}\text{C min}^{-1}$, respectively

2 MATERIALS AND METHODS

2.1 Sample

A kind of crosslinked dextrans, Sephadex G25, obtained from Amersham Pharmacia Biotech Inc. (Uppsala), was used without further purification. Size of the bead of Sepadex G25 used was $50 \sim 150\ \mu\text{m}$ in diameter. Water content of the gel was adjusted to 50 wt % as the anomalous freezing behaviour mentioned above is observed around the water content¹. For the study of Raman spectroscopy, Sephadex G100, which is another kind of dextrans with lower crosslink density than Sephadex G25 and does not indicate anomalous freezing behaviour, was also used for the comparison.

2.2 Oscillation DSC

About 10 mg of a Sephadex G25 gel with 50 wt % water content was prepared

directly in an aluminium pan and sealed hermetically. Samples were cooled from 20 °C down to - 50 °C, followed by heating to 20 °C. Cooling rate was 5 °C min⁻¹ and the following heating rate was 1 °C min⁻¹. Frequency and amplitude of the temperature oscillation during heating were 0.01 ~ 0.05 Hz and 0.5 ~ 3 °C, respectively. The instrument used was a DSC-061 (Seiko Instruments Inc., Japan).

2.3 XRD - DSC Simultaneous Measurement

Several mg of the gel was put in an aluminium pan without lid, and cooled promptly down to - 50 °C with a rate of 2 ~ 3 °C min⁻¹ followed by heating. Heating rate was 1 or 0.5 °C min⁻¹. The XRD - DSC measurement was performed with an aid of XRD-DSC II (Rigaku Corporation, Japan), where RINT Ultima⁺/HP was attached for the XRD measurement. X-ray of a 50 kV × 40 mA wavelength of Cu K_α was used. Scanning rate of diffraction angle (2θ) was 10 or 20° min⁻¹, and scanning range for 2θ was between 20° and 64° .

2.4 Raman Spectroscopy

A cuvette, outer size of which is 10 × 6.5 × 10 mm (W × D × H) with 1.25 mm in thickness, was filled with the gel of 50 wt % water, and was sealed with a teflon stopper. The cuvette, in heat-contact with a micro miniature refrigerator (MMR Technologies, Inc., USA) by one side of its surface, was set in a chamber together with the refrigerator system. The chamber with an optical window was evacuated to prevent from water condensation and ice formation on the surface of the cuvette. The cuvette containing sample was cooled from 27 °C to -40 °C in a cell holder of the Raman spectrometer and cooling rate obtained with the system was ca. 2 °C min⁻¹. The cuvette was heated subsequently to the predetermined temperature with an electric heater. Raman spectra were obtained with a Raman 960 (Thermo Nicolet, Inc., USA) where a 1064 nm YAG Laser at 450 mW was irradiated to the sample through the optical window and Raman scattering at 180° direction was observed.

3 RESULTS AND DISCUSSION

The extent of the endothermic trend starting at about -20 °C prior to the

exotherm during rewarming did not change by the oscillation DSC measurement, and was shown to be independent of frequency and amplitude of the temperature oscillation used in this study. (Figure 2) The result indicates that the trend is not of a kinetic origin due to enthalpy relaxation nor is the change in heat capacity at glass transition as the extent of the trend is too large for the change in heat capacity^{2,3}.

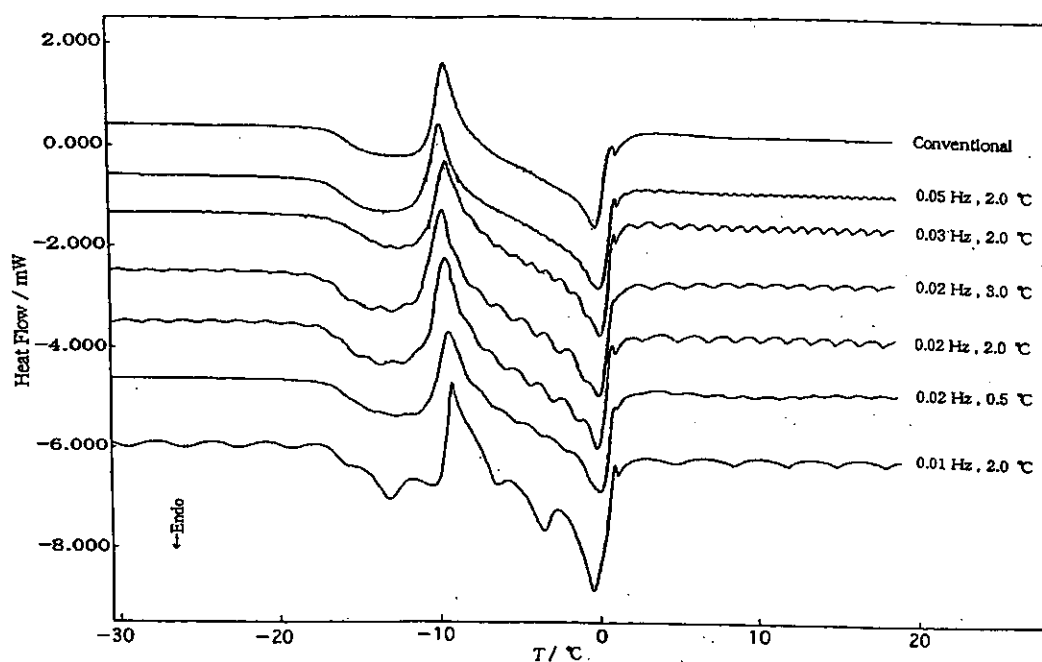


Figure 2 Heating traces obtained by oscillation DSC.

Five peaks due to ice crystal were observed between 20° and 42° for 2θ by the XRD measurement, which were all ascribed to hexagonal ice, I_h . However, diffraction at 58° , characteristic to cubic ice, I_c and presence of which is an indirect evidence for glass transition, was not observed. (Table 1) Temperature dependence of the XRD intensity was different remarkably among the three peaks between 22° and 26° , which is shown in Figures 3a and 3b. Peak 1 indicating ice crystal growth along the a axis (in the prism plane) increased most remarkably during the exotherm in the DSC rewarming trace, and second is peak 3. Peak 2 indicating ice crystal growth along the c axis, on the other hand, did not increase with the exotherm. The result might reflect a directional growth of ice crystal in the polymer network.

Table 1 *Ascription of XRD peaks.*

	2θ / deg	I_h (hexagonal ice)		I_c (cubic ice)	
		d / nm	hkl	d / nm	hkl
Peak 1	22.1~23.4	0.390	(100)		
2	23.7~24.6	0.368	(002)	0.368	(111)
3	25.3~26.4	0.344	(101)		
4	33.1~33.9	0.267	(102)		
5	39.3~40.3	0.226	(110)	0.225	(220)

$$n\lambda = 2d \sin \theta; \quad n=1; \quad d = \lambda / 2 \sin \theta; \quad \lambda = 0.15418 \text{ nm}$$

Decrease in the XRD intensity indicating the melting of ice crystal, was scarcely observed for the three peaks during the endothermic trend in the DSC scan. Therefore, it can hardly be concluded by the present study that the endothermic trend is due to the melting of ice. However, there is a possibility that decrease in the integrated XRD intensity during the endothermic trend was concealed by the integration error of the broad peak due to small ice crystal formed, overlapped with the noise level. As an another possibility, decrease in the integrated XRD intensity was concealed by the remarkable fluctuation of itself caused by the gradual melting of ice, which induces the movement of gel beads and resultant change in the angle of X-ray irradiated against the ice crystal surface. In that case, size of ice crystal might not be so small.

Assuming that the endothermic trend is due to the melting of small ice crystal, size of ice crystal can be estimated by using both Laplace and Gibbs-Duhem equations as discussed elsewhere³. Size evaluated for the radius was several nanometers. By the estimation, however, the interfacial energy between ice and hydrated dextran was assumed to be the same value as that between ice and water, 30 mJ m^{-2} , appearing in the literature⁴. Size of ice crystal can be larger actually than the estimated size as the interfacial energy between ice and hydrated dextran is expected to be larger than that between ice and water, which should be confirmed by the precise XRD study.

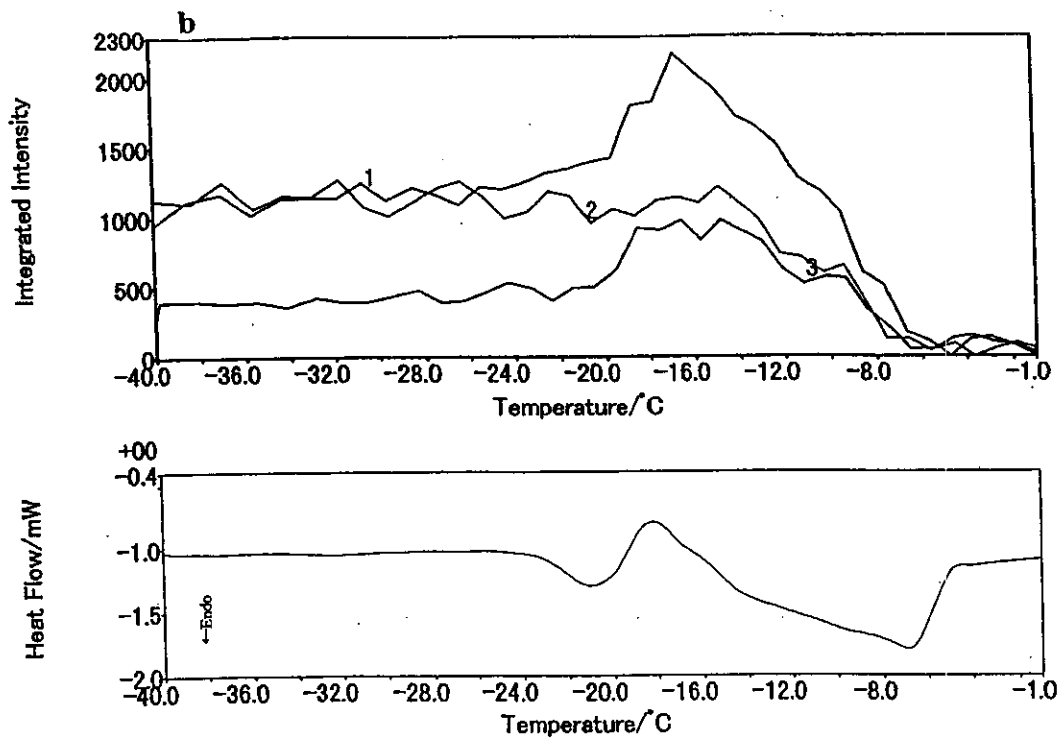
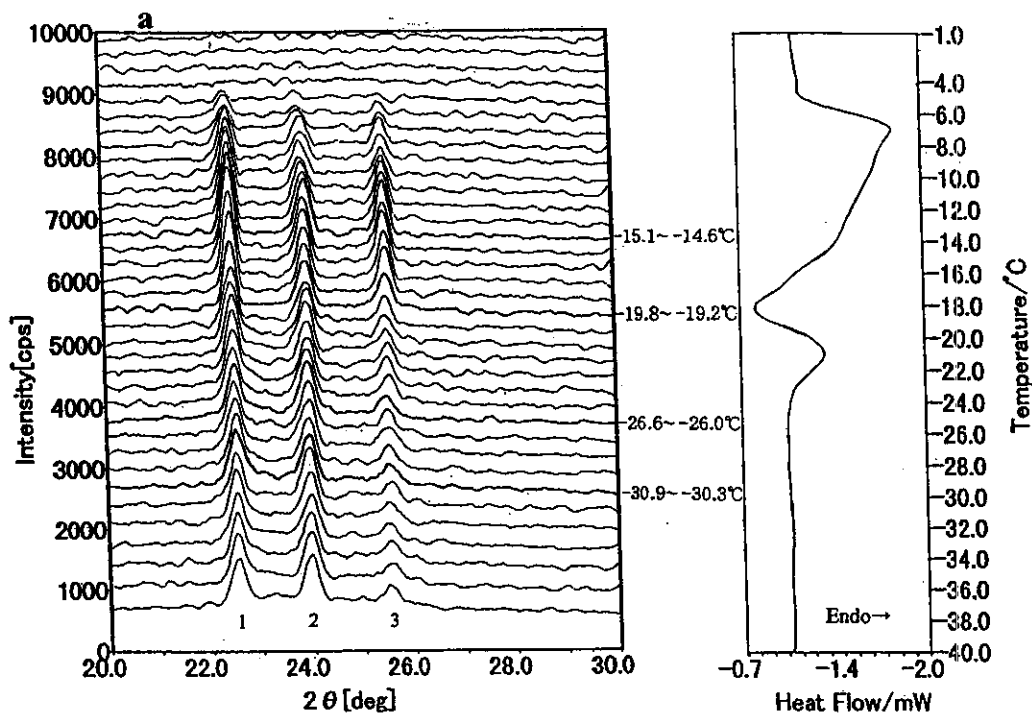


Figure 3a Heating traces obtained by the XRD-DSC measurement ; 3b Temperature dependence of the integrated XRD intensity calculated from the data shown in Figure 3a.

Raman spectra observed with a Sephadex G25 gel are shown in Figure 4a. The spectrum due to OH stretching band ($\sim 3400 \text{ cm}^{-1}$) observed at -24°C is similar to that observed at the ambient temperature, 27°C , compared with the spectrum observed at -11°C during rewarming after the occurrence of ice crystallisation. The increase in the Raman intensity in the region of lower wave number than 3400 cm^{-1} , when heated to -11°C , corresponds to the strengthening of the hydrogen bond network due to ice crystallisation. Raman spectra observed with a Sephadex G100 gel are shown in Figure 4b. The spectrum observed with the frozen gel at -40°C , on the other hand, is different from the spectrum at the ambient temperature, and is very close to the spectrum observed with a G25 gel at -11°C , shown in Figure 4a. Therefore, Raman spectra observed with the frozen G25 gel at -24°C , similar to that of the liquid water, adduces an evidence of the presence of glassy water in the frozen state of the gel.

4 CONCLUSIONS

- (1) The exotherm in the DSC rewarming trace observed with a Sephadex G25 gel, was confirmed to be due to I_h formation by the X-ray diffraction measurement. Moreover, it was found that there is a directional growth of ice crystal within the polymer gel.
- (2) However, origin of the endothermic trend, i.e., whether it is due to enthalpy relaxation at the time of glass transition, or due to the melting of small ice crystal, melting temperature being depressed by the Kelvin effect, remained still unclear.
- (3) By the Raman spectroscopic studies, presence of glassy water in the frozen state of a Sephadex G25 gel was confirmed.

ACKNOWLEDGEMENTS

The authors are most grateful to Dr. Akira Kishi, Rigaku Corporation, Japan, for the support in the X ray diffraction - DSC simultaneous measurement. They are also grateful to Mr. K. Horie for the measurement of oscillation DSC, and Mr. M. Komatsu and Mr. J. Hoshi, Thermo Nicolet Japan, Inc., Mr. A. Urata, International Servo Data Corp., and Mr. D. Terada, Nissei Science Corp. for the measurement of Raman spectra.

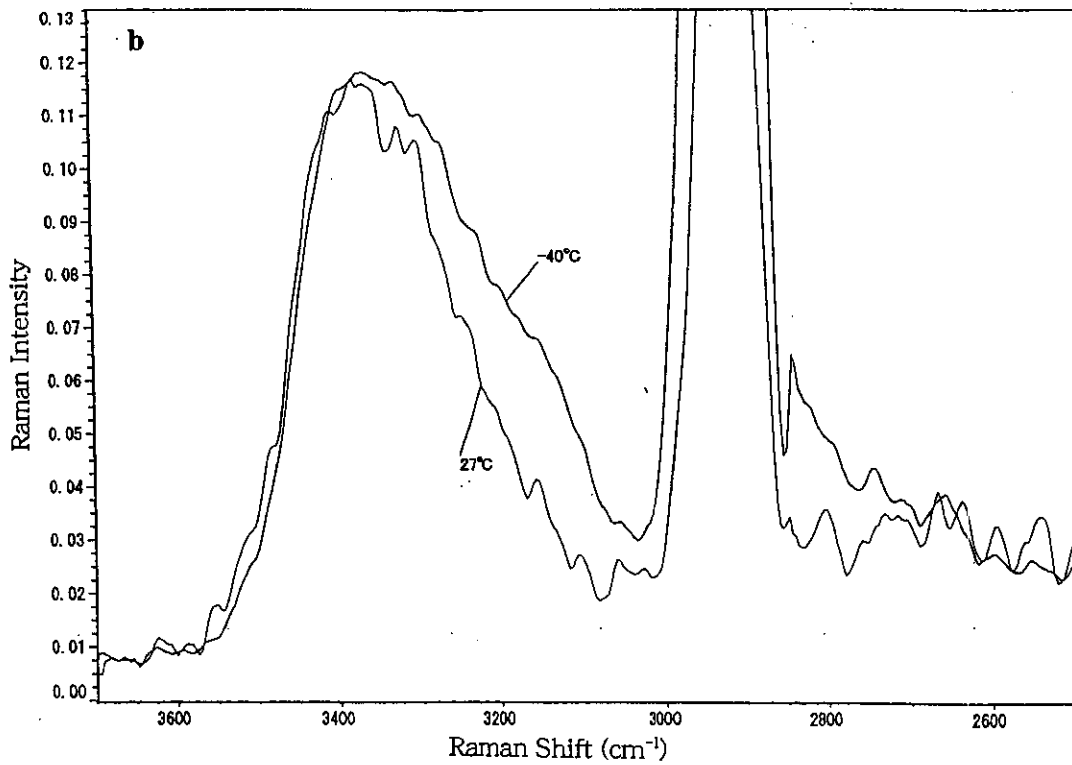
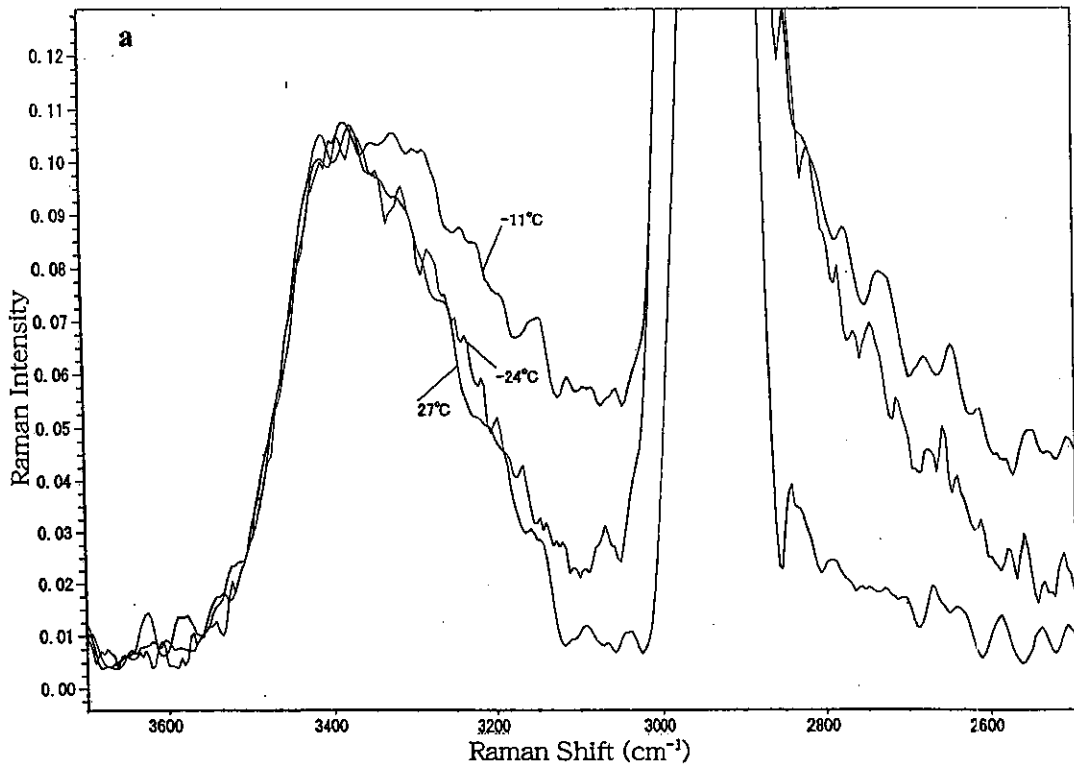


Figure 4a Raman spectra of OH stretching band observed with a Sephadex G25 gel during rewarming ; **4b** Raman spectra of OH stretching band observed with a Sephadex G100 gel.

REFERENCES

1. N. Murase, K. Gonda and T. Watanabe, *J. Phys. Chem.*, 1986, **90**, 5420.
2. N. Murase, *Cryo-Letters*, 1993, **14**, 365.
3. N. Murase, T. Inoue and M. Ruike, *Cryo-Letters*, 1997, **18**, 157.
4. K.L. Kerr, R.E. Feeney, D.T. Osuga and D.S. Reid, *Cryo-Letters*, 1985, **6**, 371.

20010976

以降は雑誌/図書等に掲載された論文となりますので
「研究成果の刊行に関する一覧」をご参照ください。